Bi/BiOI/Carbon quantum dots nano-sheets with superior photocatalysis

Chenhui Zhao[a], Zhijie Zhao[a], Ying Liang,[b] and Jiangfeng Fu[a*1]

[a]School of Power and Energy, Northwestern Polytechnical University, Xi'an 710072, China

[b]School of Chemistry and Chemical Engineering, Northwestern Polytechnical University, Xi'an 710072, China

2. Experimental section

2.1. Photocatalyst synthesis

All chemicals were purchased from J&K Chemical and used as received. The BiOI microspheres were synthesized by a facile solvo-thermal method. In a typical procedure, 5.35 g $Bi(NO_3)_3 \cdot 5H_2O$ and 1.8 g KI was dissolved in 80 mL of ethylene glycol by ultra-sonic. Then, the solution was transferred into a 100 mL teflon-lined stainless-steel autoclave and kept at 180 °C for 8 h. After the reaction finished, the resulting samples were collected and separated by centrifugation and washed with deionized water and absolute ethanol followed by drying via the vacuum freeze-drying technology.

The synthesis of BiOI/CQDs materials was carried out as follows. Firstly, 1.0 g as-prepared BiOI microspheres were dispersed in 80 mL deionized water by ultrasonic for about 5 min. Then the stoichiometric (0.2 g, 0.4 g, and 0.6 g) citric acid and 2.68 mL ethylenediamine was added into the above system under continuous mechanical stirring. The above mixture was transferred into 100mL teflon-lined stainless-steel autoclave and heated at 180 °C for 8 h and cooled down to room temperature. The acquired product was subjected to centrifugation and washed several times with deionized water and absolute ethanol followed by drying via the vacuum freeze-drying technology centrifugation. The resulting sample was coded as BiOI/CQDs-α, and α denotes the mass of citric acid.

[1]* Corresponding author at: School of Power and Energy, Northwestern Polytechnical University, Xi'an 710072, China. E-mail addresses: fjf@nwpu.edu.cn(J. Fu).

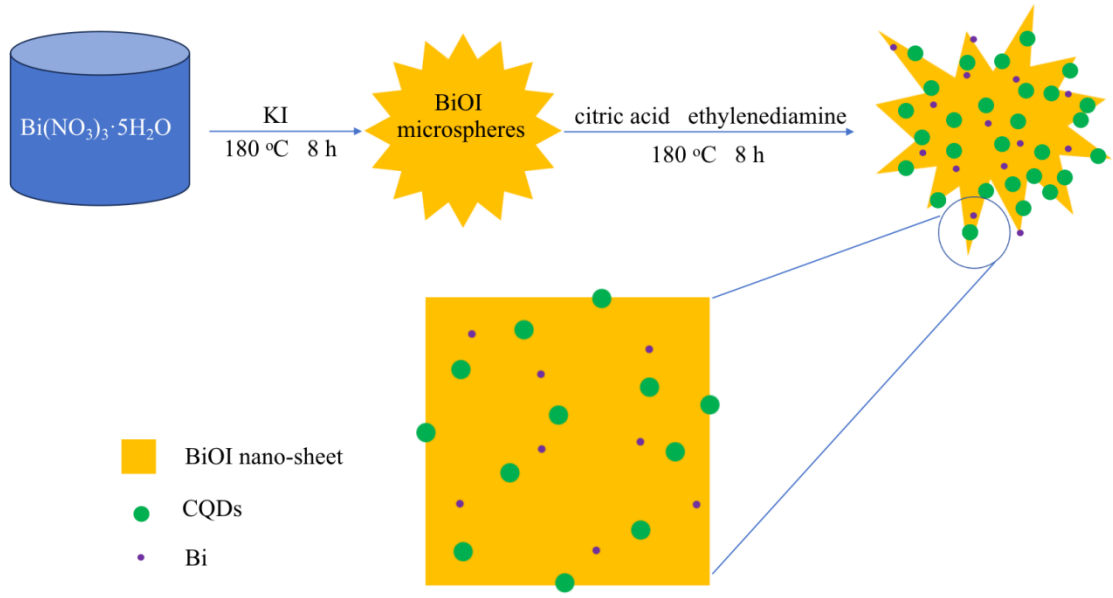

Fig. S1 Schematic illustration of the synthesis of the Bi/BiOI/CQDs photocatalyst

2.2. Photocatalyst characterization

The crystalline phases of Bi/BiOI/CQDs materials were deter- mined by X-ray power diffraction (XRD) analysis using a Bruker AXS D8-advance X-ray diffractometer with Cu-K radiation. The elements and chemical states on the surface of BiOI/CQDs materials were determined by X-ray photoelectron spectroscopy (XPS) using an Axis Ultra instrument (Kratos Analytical, Manchester, U.K.) under ultrahigh vacuum condition ($<10^{-6}$ Pa) with a monochromatic Al K X-ray source (1486.6 eV). Fourier transform-infrared (FT-IR) spectra were measured on a PerkinElmer 580BIR spectrophotometer using KBr pellet technique. Thermogravimetric analysis (TG) was performed on a Q5000IR (TA Instruments, US) apparatus. Scanning electron microscopy (SEM) micrographs were observed on a JEOL-JSM-6700F. Transmission electron microscopy (TEM) micrographs were observed on a JEOL JEM-2100F. N_2 adsorption/desorption isotherms were obtained on a TriStar II 20 apparatus. UV–vis diffuse reflectance spectra (DRS) were per-formed on a Shimadzu UV-3600 spectrometer ($BaSO_4$ power as substrate). The Photoluminescence (PL) spectra of BiOI/CQDs materials were detected on a Varian Cary Eclipse spectrometer.

2.3. Photocatalytic activity test

The photocatalytic activity of the as-prepared Bi/BiOI/CQDs materials with different CQDs contents was investigated by the photodegradation of 20 mg/L RhB under visible light (a 300 W Xe arc lamp with a UV cutoff filter (400 nm)). In a typical process, 100 mg BiOI/CQDs samples were added into 100 mL RhB. Prior to irradiation, the suspension was stirred in the dark for 30 min to

ensure adsorption-desorption equilibrium. During the photo-degradation process, 3 mL suspension was sampled at certain time intervals and centrifuged at 13000 rpm for 3min to remove the Bi/BiOI/CQDs microspheres for analysis. The concentration of RhB samples were analyzed on an UV–vis spectrophotometer (UV-2450, Shimadzu) at wavelength of 553 nm.

2.4. Free radical trapping experiments

For detecting the active species during photocatalytic reactivity, hydroxyl radicals (·*OH*), superoxide radicals ($O_2^{\bullet-}$), holes (h^+) and electrons (e^-) were investigated by adding 1.0 mM IPA (a quencher of ·*OH*), 1 mM p-benzoquinone (BQ, a quencher of $O_2^{\bullet-}$), 1 mM KI (a quencher of h^+) and 1 mM tertiary butanol (TBA) for e^-, respectively. The method was similar to the former photocatalytic activity test.

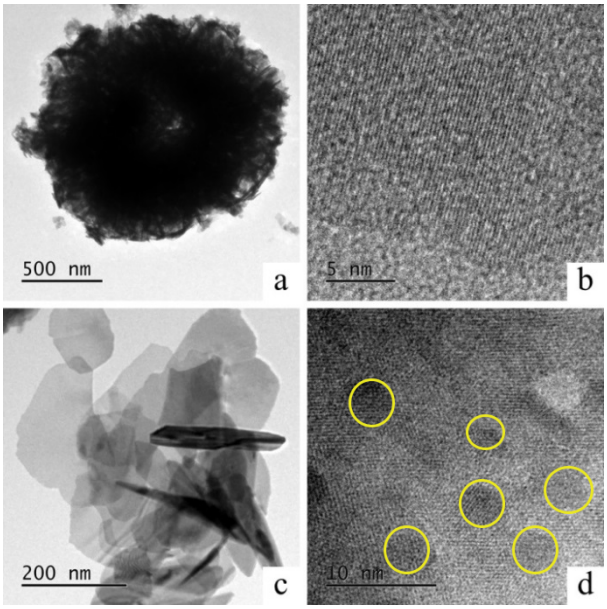

Fig. S2 TEM images of Bi/BiOI/CQDs

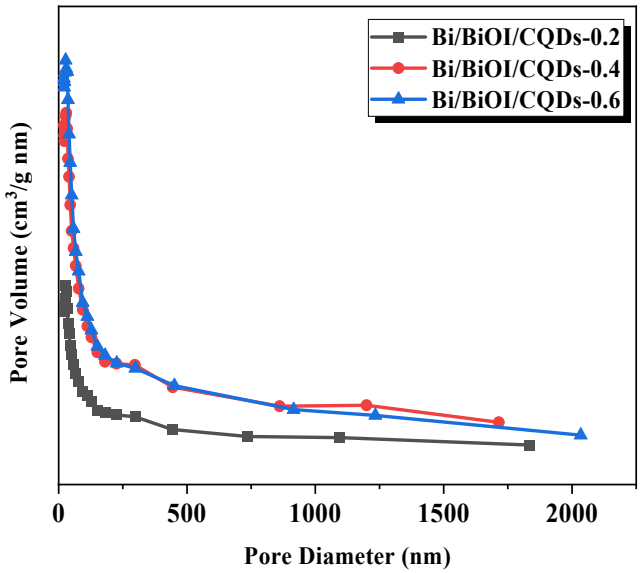

Fig. S3 Pore size distribution curves of Bi/BiOI/CQDs with different CQDs amounts

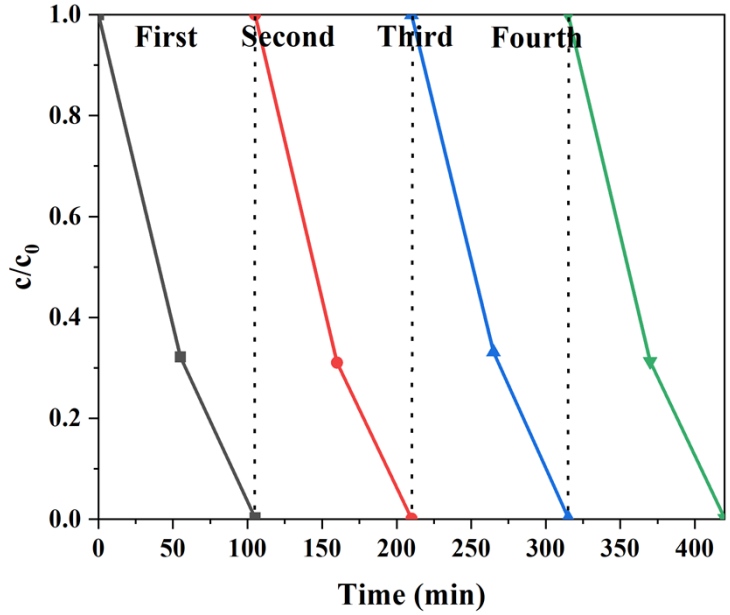

Fig. S4 Cycling runs for the photodegradation of RhB by Bi/BiOI/CQDs materials under visible light irradiation

Table S1 The comparison of this work with recent reported Bi-based catalysts for photodegradation

Name	Morphology	Pollutant	Degradation rate	Reaction condition	Ref
Bi/BiOBr	Pine Dendritic	tetracycline	75.8% achieved in 30 min	Initial concentration: 20mg/L; 300 W Xe solar simulator lamp	[1]
g-C_3N_4@Bi/BiOI	3D fluffy and hierarchical structure	Hg^0	73.85% attained in 40 min	Initial concentration: 58 μg/m^3; 9 W LED irradiation	[2]
Bi-BiOI/graphene	uniform 3D microspheres	NO	51.8% achieved in 30 min	300 W Xenon lamp under 600 nm cut-off filters light irradiation	[3]
Bi@BiOI-Bi_2O_3/C_3N_4	film	Cr (VI) and phenol	100% achieved in 1.5 h	Initial concentration: phenol and Cr(VI) were 5 mg /L and 8×10^{-5} mol/L, respectively; 300 W Xe lamp	[4]
Bi/BiOI-Bi_2O_3	layered structure	phenol	100% achieved in 3.5 h	Initial concentration: 5	[5]

	with sheet			mg/L; 300 W Xenon lamp	
Bi/BiOI	3D fower-like sharp	microcystin-LR	68.7% achieved in 2 h	350 W Xe lamp	[6]
Bi/BiOCl-TiO_2-CQDs	lamellar structure	methyl orange (MO) and p-nitrophenol (PNP)	94% of MO attained in 100 min and 82% of PNP in 240 min	Initial concentration: 20 mg/L 500 W xenon lamp	[7]
Bi/BiOBr	hollow hierarchical microspheres	rhodamine B (RhB)	89.49% in 45 min	filter 420 nm xenon lamp	[8]
Bi/BiOCl/$Bi_2O_2CO_3$	irregular loose spherical block structure	RhB	99.0% in 12 min	Initial concentration:100 ppm 300 W Xe lamp	[9]
Bi/BiOCl	nanosheets	RhB	98% in 120 min	Initial concentration: 20 mg/L 500W Xe lamp	[10]
Bi/BiOCl	flowerlike	RhB	98.7% in 200 s	Initial concentration: 20 mg/L 300 W Xe light	[11]
g-C_3N_4@Bi/BiOBr	3D fluffy and hierarchical structure	RhB and tetracycline	98% of RhB in 80 min and 78% of tetracycline in 4 h	Initial concentration: rhodamine B and Tetracycline were 20 mg/L and 12 mg/L, respectively;	[12]
Bi/BiOBr	microspheres	Cr(VI) and RhB	95% of Cr(VI) in 180 min, 98% of RhB in 60 min	Initial concentration: Cr(VI) and RhB were 20 mg/L and 8 mg/L, respectively; 500 W xenon lamp	[13]
$CuBi_2O_4$/Bi/BiOBr	hierarchical structure	ciprofloxacin (CIP) and Methylene blue (MB)	81% and 73% in 120 min	Initial concentration: 20 mg/L;500 W Xenon lamp	[14]
Bi_2S_3/Bi/BiOBr	hierarchical structure	Cr(VI)	95.82 % in 2 h	Initial concentration: 10 mg/L; 300 W	[15]

Co-doped Bi/BiOBr	nanosheet	bisphenol A (BPA)	94% in 30 min	xenon lamp Initial concentration: 1 mg/L; 300 W xenon lamp	[16]

[1]. Li, W., et al., Pine Dendritic Bi/BiOBr Photocatalyst for Efficient Degradation of Antibiotics. Langmuir, 2023. 39(11): p. 4140-4149.

[2]. Wang, R., et al., Bi spheres decorated g-C_3N_4/BiOI Z-scheme heterojunction with SPR effect for efficient photocatalytic removal elemental mercury. Applied Surface Science, 2021. 556.

[3]. Zhu, G., et al., Enhancing visible-light-induced photocatalytic activity of BiOI microspheres for NO removal by synchronous coupling with Bi metal and graphene. Applied Surface Science, 2019. 467-468: p. 968-978.

[4]. Du, H., et al., Exceptional visible-light photoelectrocatalytic activity of dual Z-scheme Bi@BiOI-Bi(2)O(3)/C(3)N(4) heterojunction for simultaneous remediation of Cr(VI) and phenol. J Colloid Interface Sci, 2023. 640: p. 132-143.

[5]. Wang, Q., et al., Fabrication of visible-light-active Bi/BiOI-Bi(2)O(3) composite with enhanced photocatalytic activity. J Colloid Interface Sci, 2019. 548: p. 255-264.

[6]. Xiao, F., et al., Construction of oxygen vacancy modified Bi/BiOI nanocomposite with improved photocatalytic activity for microcystin-LR degradation. Journal of Materials Science: Materials in Electronics, 2020. 31(19): p. 17003-17012.

[7]. Li, W., C. Zhao, and Q. Zhang, Synthesis of Bi/BiOCl-TiO_2-CQDs quaternary photocatalyst with enhanced visible-light photoactivity and fast charge migration. Catalysis Communications, 2018. 107: p. 74-77.

[8]. Zhang, X., et al., The role of Sn in enhancing the visible-light photocatalytic activity of hollow hierarchical microspheres of the Bi/BiOBr heterojunction. Phys Chem Chem Phys, 2015. 17(12): p. 8078-86.

[9]. Wang, L., et al., Ni2+-assisted catalytic one-step synthesis of Bi/BiOCl/$Bi_2O_2CO_3$ heterojunction with enhanced photocatalytic activity under visible light. Applied Catalysis B: Environmental, 2022. 305.

[10]. Yu, Y., et al., One-step solution combustion synthesis of Bi/BiOCl nanosheets: Reaction mechanism and photocatalytic RhB degradation. Journal of Physics and Chemistry of Solids, 2023. 174.

[11]. Wang, S., et al., Controlled preparation of Bi/BiOCl with enhanced catalytic activity for organic pollutant under visible light using one-pot hydrothermal technology. Chemosphere, 2022. 307(Pt 4): p. 136188.

[12]. Liu, H., et al., Engineering design of hierarchical g-C_3N_4@Bi/BiOBr ternary heterojunction with Z-scheme system for efficient visible-light photocatalytic performance. Journal of Alloys and Compounds, 2019. 798: p. 741-749.

[13]. Wang, Y., et al., Hierarchical Bi-doped BiOBr microspheres assembled from nanosheets with (0 0 1) facet exposed via crystal facet engineering toward highly efficient visible light photocatalysis. Applied Surface Science, 2020. 514.

[14]. Fu, S., et al., Construction of hierarchical $CuBi_2O_4$/Bi/BiOBr ternary heterojunction with Z-scheme mechanism for enhanced broad-spectrum photocatalytic activity. Journal of Alloys and Compounds, 2021. 878.

[15]. He, R., et al., Tunable Bi-bridge S-scheme Bi_2S_3/BiOBr heterojunction with oxygen vacancy and SPR effect for efficient photocatalytic reduction of Cr(VI) and industrial electroplating wastewater treatment. Separation and Purification Technology, 2023. 311.

[16]. Wang, Q., et al., Enhanced visible-light driven photocatalytic degradation of bisphenol A by tuning electronic structure of Bi/BiOBr. Chemosphere, 2022. 308(Pt 2): p. 136276.